Thermal Radiation Model for Solid Rocket Booster Plumes

G.H. Watson* and A.L. Lee†
Lockheed Missiles & Space Company, Inc., Huntsville, Ala.

The Monte Carlo method is used to model the thermal radiation field of the plumes for the dual solid rocket boosters astride the Space Shuttle launch configuration. The model accounts for axial and radial variations in radiative properties of the plumes. The plumes are considered to be composed of a dispersion of aluminum oxide (Al_2O_3) particles immersed in the gaseous products of combustion. The principal emitting gases are taken to be CO, CO_2, H_2O, and HCl. The thermal model is based on local thermodynamic equilibrium. Scattering of radiant energy by Al_2O_3 particles may be treated as isotropic or anisotropic. Sample radiant heating rates to the base region of the Space Shuttle are shown. Space Shuttle geometries are simulated as combinations of quadric surfaces.

Nomenclature

A = area
A/E = absorption to extinction ratio
$C_1,\ldots,C_{10}$ = quadric coefficients
d = length parameter
E_b^g = blackbody emissive power for gas
E_b^p = blackbody emissive power for particles
e = energy content of bundles
f = mole fraction
H = elevation of axial region boundary
I = radiation intensity
J = volumetric emission of radiant energy
K = linear absorption coefficient for gas
M = Mach number
N = particle number density
N_e = sample size for energy bundles
N_h = number of energy bundles striking a surface
N_{re} = number of re-emissions
P = property
p = pressure
q = heating rate
R = distance from plume vertex to line of sight
r = radial coordinate
R_{ex} = nozzle exit radius
S = length of travel
S_p = probable length of travel
$S(\eta)$ = scatter function
T = temperature
U = random number
$u_{1,2,3}$ = direction cosines
V = volume
X_1,X_2,X_3 = principal Cartesian coordinates
X',X'',X''' = principal coordinates of line of sight
Z = axial coordinate
α = gimbal angle in pitch plane
β = angle between r_1 and r_2
γ = cone half-angle
ξ = angle between ϕ_1 and ϕ_2
η = polar angle for line of sight
θ = azimuth angle for line of sight
ψ = gimbal angle in yaw plane
$\sigma_{a,e}$ = absorption extinction cross sections
τ = optical depth
λ = wavelength

Superscripts and Subscripts

$(\bar{\ })$ = gray property
g = gas
i = index for axial region boundary
j = index for radial region boundary
n = index for regions
0 = initial
p = particles
1 = present event site
2 = new event site
∞ = freestream

Received Jan. 31, 1977; revision received June 29, 1977.
Index categories: Radiation and Radiative Heat Transfer; Thermal Modeling and Analysis.

*Currently Staff Scientist, Oak Ridge National Laboratory, Oak Ridge, Tenn.
†Scientist Associate Research. Member AIAA.

Introduction

THERMAL radiation from exhaust plumes of the solid rocket boosters (SRB) astride the Space Shuttle ascent phase configuration is a major contributor to base heating. A thorough treatment of SRB thermal radiation must consider the influences of plume flowfield structure on the magnitude and spatial distribution of thermal radiation leaving the plume. SRB plumes are composed of a dispersion of Al_2O_3 particles distributed throughout the gaseous products of combustion of the solid propellant. The principal emitting gases in the products of combustion of the plume are CO, CO_2, H_2O, and HCl. Thermal radiation from Al_2O_3 dispersions in SRB plumes have been approximated by simulating the plume as a homogeneous cloud of hot Al_2O_3 particles.[1,2] Axial variations in Al_2O_3 particles were considered in Ref. 3, wherein uncoupled thermal radiation from the Al_2O_3 particles and emitting gases was approximated. The SRB thermal radiation model documented in Ref. 4 and discussed in this paper allows the prediction of radiant heating rates as influenced by spatial variations in the properties of the Al_2O_3 particles, and emitting gases dictated plume flowfield structure. The model considers both SRB plumes that may be gimbaled independently in the yaw and pitch planes. Shuttle geometries in the base region are simulated as quadric surfaces, which may be assembled in combination for accurate representation of the actual vehicle. The Monte Carlo method is used to solve the radiation transport problem, so that the influences of surface shading are accounted for inherently and accurately.

The SRB plume thermal radiation model discussed herein was developed principally to delineate the influence of plume flowfield structure on the magnitude and distribution of thermal radiation leaving the plume. To expedite this end, the SRB plumes are modeled as gray media in local thermodynamic equilibrium. The resulting mathematical model can be used to gage the effects of plume flowfield structure as influenced by such parameters as altitude, Mach number, and propellant combustion products.

Flowfield Model

A number of parameters influence the SRB plume flowfield structure. The more influential are chamber pressure, ambient pressure, Mach number of the approaching flow, and afterburning. The effects of these parameters on the plume structure may be predicted by two-phase flowfield calculation methodologies.[5] The flowfield properties that must be supplied to the thermal radiation model are particle number density, particle temperature, particle radius, gas temperature, gas pressure, and mole fractions for CO, CO_2, H_2O, and HCl. The SRB plumes are assumed to be axisymmetric. The axial and radial variations in these plume properties are delineated for the SRB thermal radiation model by a lattice of grid points at the intersections of an array of conical surfaces emanating from a common vertex and a series of planes at right angles to the plume axis (Fig. 1). Each region of the plume is considered to be homogeneous, and the plume properties are defined by Eq. (1), wherein linear variations in properties are assumed across the region:

$$\bar{P}=\int_V P(r,Z)\,\mathrm{d}V \Big/ \int_V \mathrm{d}V \tag{1}$$

The SRB thermal radiation model provides the capability to calculate radiant heating rates from single plumes or from the dual plumes astride the external tank of the Space Shuttle. In the dual-plume calculation, the dual plumes are defined in a central Cartesian coordinate system (X_1,X_2,X_3) centered equidistant between the two SRB nozzles. Both plumes are axisymmetric, with identical flowfields. The plumes may be gimbaled independently of one another in both yaw and pitch planes, and the dual plumes may or may not intersect, depending on plume expansion.

SRB Plume Thermal Radiation

Under conditions of local thermodynamic equilibrium (LTE), the spectral radiant energy emitted by a homogeneous volume of particles and gas may be expressed as[4]

$$J_\lambda = 4V(N\sigma_{a,\lambda}E^p_{b,\lambda} + K_\lambda E^g_{b,\lambda}) \tag{2}$$

To simplify the model, the variation of plume radiative properties over the wavelength spectrum is approximated with gray values. Planck mean absorption coefficients are used for the gases and Al_2O_3 particles. Gray volumetric absorption coefficients for CO, CO_2, and H_2O are presented in Ref. 6 as functions of temperature properties of the gases at atmospheric pressure. The Planck mean absorption coefficient for HCl is comparable to that of CO. The Planck mean coefficient for the gaseous mixture of CO, CO_2, H_2O, and HCl is then represented as

$$\bar{K}_{a_{\text{mixture}}} = \frac{p}{1\ \text{atm}} \sum_{m=1}^{4} \bar{K}_m f_m \tag{3}$$

Planck mean absorption cross sections for the dispersion of Al_2O_3 particles in the SRB plume are calculated by numerically evaluating the integrals in Eq. (4). The spectral dependence of $\sigma_a(\lambda)$ and $\sigma_e(\lambda)$ is defined by the Mie theory solution documented in Ref. 2:

$$\bar{\sigma}_a, \bar{\sigma}_e = \frac{\int_0^\infty \sigma_a(\lambda), \sigma_e(\lambda) E_b(\lambda,T)\,\mathrm{d}\lambda}{\int_0^\infty E_b(\lambda,T)\,\mathrm{d}\lambda} \tag{4}$$

An index of refraction for Al_2O_2 of $1.8 + 0.005i$ was used in the Mie theory calculations for $\sigma_a(\lambda)$ and $\sigma_e(\lambda)$, as recent data indicate that solid Al_2O_3 particles exhibit absorption properties close to those of liquid Al_2O_3.[7]

The gray approximation to the total radiation emitted by the entire volume of the plume then is taken to be the sum of the radiant energy emitted by all regions of the plume[4]:

$$J_{\text{total}} = 4 \sum_{n=1}^{\text{all regions}} (N\bar{\sigma}_a E^p_b|_n + \bar{K} E^g_b|_n)\, V_n \tag{5}$$

Monte Carlo Model

The distribution of thermal energy leaving the plume is calculated using a Monte Carlo technique. The solution to the radiation transport problem is effected by following energy bundles (which may be considered to be large groups of photons) as they are emitted, scattered, and absorbed (and re-emitted as required by LTE) in the same manner as photons until they leave the plume. Upon leaving the plume boundary, the energy bundle is tracked to determine if the bundle path intersects a target surface of interest. If the bundle strikes a target surface of interest. If the bundle strikes a target surface, a portion or all of the energy contained in the bundle will contribute to the surface radiant heat load,[4] depending on how the absorbing properties of the surface are modeled. The radiant heat flux to a given surface is ultimately determined by tabulating the number of bundles striking a surface relative to the total number of bundles leaving the plume.

The amount of energy contained in an energy bundle for a specific SRB plume is dependent on the number of samples N_e and the number of absorption/re-emission events, N_{re} which occur during the simulation. The energy per bundle e is related to the number of emissions in a plume region by taking the number of samples N_e occurring in the region plus the number of re-emissions in the region after absorbing bundles originating at other event sites.[8] The energy per bundle is defined by Eq. (6), which considers energy emitted by the entire plume:

$$(N_e + N_{\text{re}})e = 4 \sum_{n=1}^{\text{all regions}} (N\bar{\sigma}_a E^p_b|_n + \bar{K} E^g_b|_n)\, V_n \tag{6}$$

Equation (6) defines the energy per bundle e for a specified sample size N_e, and the heat flux to a given surface is calculated from

$$q = N_h e / A \tag{7}$$

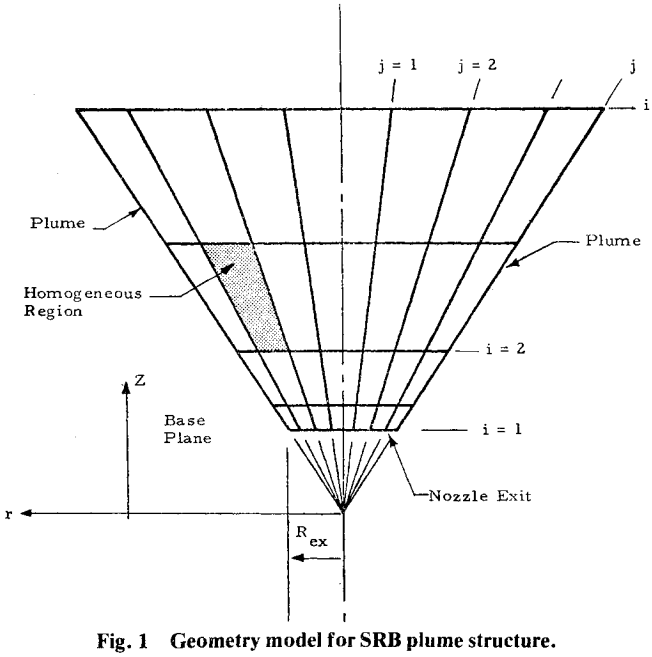

Fig. 1 Geometry model for SRB plume structure.

Each region of the plume emits thermal radiation as defined by Eq. (5), wherein the magnitude of the emitted radiation is dependent on the particle number density, gas density, the volume of the region, and the fourth power of gas and particle temperature. All energy bundles have equal energy. However, since various regions emit varying amounts of thermal radiation, depending on the aforementioned variables, the strongly emitting regions will be assigned correspondingly larger numbers of bundles. In this manner, the distribution of emitted thermal radiation throughout is approximated. For a given sample size N_e, the number of spontaneous emissions that are allowed to take place in a given region is determined by the fraction of the total energy emitted by the plume which is emitted by the given region as

$$N_{e_n}/N_e = J_n/J_{\text{total}} \tag{8}$$

where N_e is the total number of bundles emitted by the entire plume, and N_{e_n} is the number of bundles emitted by region n. Once the region in which the emission is to take place has been selected, it is necessary to assign the location of the emission site within the region. Since each region is homogeneous, it is required that the ratio of the number of emission event sites in the volume element dV to the total number of emission sites in the region N_{e_n} be identical to the ratio of dV to volume of the region, V:

$$\frac{dN_e}{N_e} = \frac{dV}{V} = \frac{r\,dr\,d\phi\,dZ}{V} \tag{9}$$

The volume of a region of the plume may be expressed as

$$V = \int_0^{2\pi}\int_{H_i}^{H_{i+1}}\int_{z\tan\gamma_j}^{z\tan\gamma_{j+1}} r\,dr\,d\phi\,dz$$

$$= \pi(\tan^2\gamma_{j+1} - \tan^2\gamma_j)\frac{(H_{i+1}^3 - H_i^3)}{3}$$

Then

$$\frac{dN_e}{N_e} = \frac{dV}{V} = \frac{2r\,dr}{Z^2(\tan^2\gamma_{j+1} - \tan^2\gamma_j)}\,\frac{d\phi}{\pi}\,\frac{3Z^2\,dZ}{H_{i+1}^3 - H_i^3} \tag{10}$$

which may be taken to be the joint probability density function for the selection of emission sites within a given plume region. The coordinates for the random selection of emission sites within a region devolve from Eq. (10) as

$$\phi = 2\pi U_\phi \tag{11}$$

$$Z = [(H_{i+1}^3 - H_i^3)U_z + H_i^3]^{1/3} \tag{12}$$

$$r = Z\sqrt{U_r(\tan^2\gamma_{j+1} - \tan^2\gamma_j) + \tan^2\gamma_j} \tag{13}$$

where U is a random number between 0 and 1 with uniform distribution.

After an emission site has been selected, it is necessary to select the direction of travel for the subject energy bundle in a spherical coordinate system centered at the emission event site. Coordinate selection for the direction of travel (the line of sight) for spontaneous emission and isotropic scattering are taken from Ref. 9 as

$$\cos\eta = 1 - 2U_\eta \tag{14}$$

$$\theta = 2\pi U_\theta \tag{15}$$

for the polar and azimuthal angles, respectively.

The anisotropic scattering nature of Al_2O_3 particles may also be simulated using the Monte Carlo method in the manner outlined in Ref. 1, wherein the integral of the scatter function, defined by Mie theory, is approximated by the normalized area under a curve of $S(\eta)\sin\eta$ vs η and set equal to a random number:

$$\int_0^{\eta} S(\eta)\sin\eta\,d\eta = U_\eta \tag{16}$$

Equation (16) implicitly defines the polar angle for anisotropic scattering of unpolarized radiation, whereas Eq. (15) may be used to define the azimuth angle of scatter.

For a homogeneous region of the SRB plume, the attenuation of gray radiation may be expressed as

$$I/I_0 = \exp[-N\bar{\sigma}_a + \bar{K})S] \tag{17}$$

and the fraction of intensity removed prior to x is

$$1 - (I/I_0) = 1 - \exp[-(N\bar{\sigma}_a + \bar{K}_a)x] \tag{18}$$

where x is used here as an independent variable defining a point along the line of sight. As discussed in Ref. 9, Eq. (18) can be thought of as the probability that the actual (or probable) length of travel S_p within the region will be less than x. This consideration allows the random selection of probable lengths of travel for an energy bundle within the plume before an absorption or scatter event occurs. The probable length of travel for an energy bundle may take it across several different homogeneous regions before it either encounters a scatter or absorption event or escapes the plume. Each region of the plume has its own unique optical properties and attenuates the radiation intensity passing through it at different rates. Consider a beam of radiation passing through a series of homogeneous media with varying optical properties. The length of travel in each region and the optical properties of the region define the rate of attenuation of radiant energy from the beam.

The attenuation from the event site at $S=0$ to any station along the line of sight is expressed as

$$I/I_0 = \exp[-(\tau_1 S_1 + \tau_2 S_2 + \cdots + \tau_n S_n)]$$

where $\tau = \tau_p + \tau_g = (N\bar{\sigma}_a + \bar{K})R_{\text{ex}}$ and $S_{1,2,\ldots,n}$ are nondimensionalized with R_{ex}. The probability of collision along the line of sight is

$$1 - (I/I_0) = 1 - \exp\{-(\tau_1 S_1 + \tau_2 S_2 + \cdots + \tau_{n-1} S_{n-1}$$

$$+ [S_p - (S_1 + S_2 + \cdots + S_{n-1})]\tau_n)\} = U_s$$

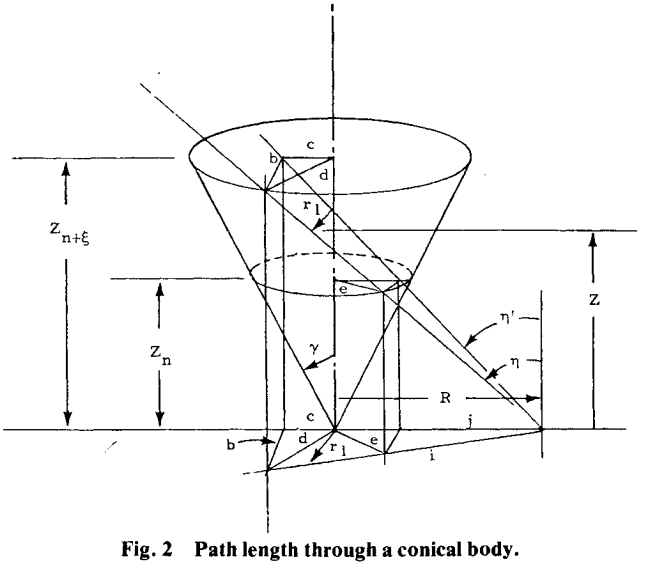

Fig. 2 Path length through a conical body.

and, solving explicitly for S_p in the nth region,

$$S_p = \sum_{k=1}^{n-1} S_k - \frac{\ell n U_S + \sum_{k=1}^{n-1} \tau_k S_k}{\tau_n} \tag{19}$$

where n regions are traversed. An event occurs in the nth region if the probable length of travel S_p along the line of sight is less than the maximum length S within the nth plume region along the line of sight. If S_p is greater than S_n, the radiation intensity is attenuated by $\tau_n S_n$, and S_p for region $n+1$ is calculated as per Eq. (19). If the nth region is at the plume boundary and S_p is greater than S, the bundle will leave the plume.

When the length of travel to an event site has been determined, it is necessary to determine whether an absorption or scatter event occurs. This is done by comparing the absorption/extinct ratio A/E for the local medium to a randon number, where

$$\frac{A}{E} = \frac{\bar{\sigma}_a/\bar{\sigma}_e \tau_p + \tau_g}{\tau} \tag{20}$$

It is necessary to derive expressions for the true lengths along the line of sight subtended by each plume region intersected in order to define attenuation along the line of sight. The true length of travel S_n in region n is

$$S_n = \frac{Z_{n+1} - Z_n}{\cos\eta} \tag{21}$$

where Z_n is the Z coordinate of successive intersections of the line of sight and region boundaries. The intersection may occur on the horizontal planes or the conical boundaries defining the region. If a horizontal plane boundary is intersected, the value Z_n is known. When a conical boundary is intersected, Z_n is calculated from a modified version of the method used in Ref. 10:

$$Z_n = \{\tan\gamma + R\tan\eta' \pm [(\tan\gamma + R\tan\eta')^2 + (1-R^2)(\tan^2\eta - \tan^2\gamma)]\}^{1/2} \times (\tan^2\eta - \tan^2\gamma)^{-1} \tag{22}$$

Equation (22) is derived from geometric considerations of the line of sight and conical boundary shown in Fig. 2.

As the energy bundles are emitted, scattered, absorbed, and re-emitted throughout the plume, their locations are tracked in a cylindrical coordinate system (r, Z, ϕ) centered at the plume vertex with the Z axis aligned with the plume axis. The Z coordinate of the new event site is (see Fig. 3)

$$Z_2 = Z_1 + S_p \cos\eta \tag{23}$$

The new value for the r coordinate is obtained from the law of cosines (see Fig. 3):

$$r_2 = \sqrt{r_1^2 + (S_p \sin\eta)^2 - 2 r_1 S_p \sin\eta \cos[\pi - (\theta - \phi_1)]} \tag{24}$$

and ϕ is updated as

$$\phi_2 = \phi_1 \pm \xi \tag{25}$$

where

$$\xi = \cos^{-1}\left(\frac{\sqrt{r_1^2 + r_2^2 - (S_p \sin\eta)^2}}{2 r_1 r_2}\right) \tag{26}$$

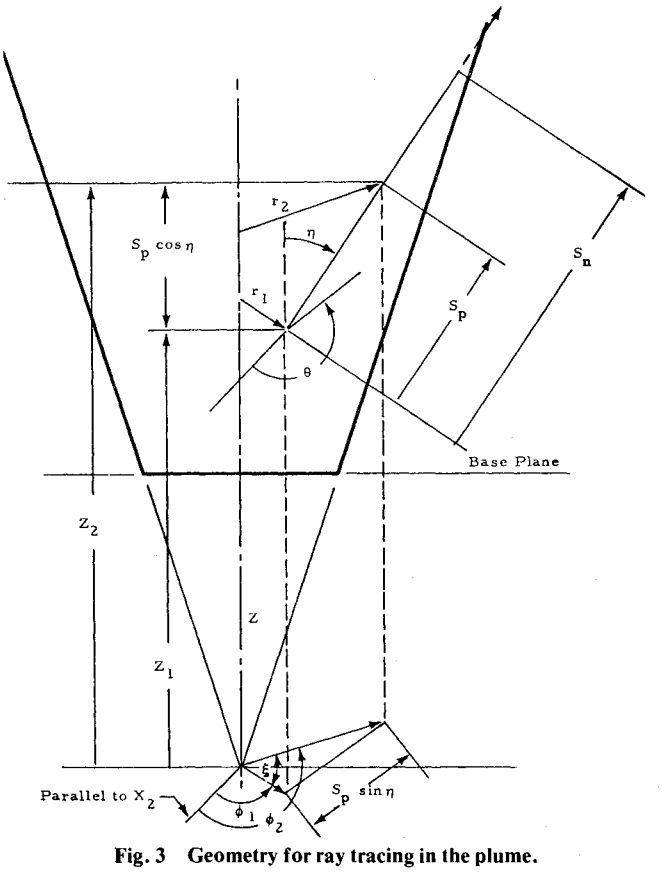

Fig. 3 Geometry for ray tracing in the plume.

Energy bundles are tracked through the plume from event to event until they leave the plume boundary. When a bundle exits one SRB plume, the line of sight along which the bundle is traveling is represented as a linear algebraic expression that is checked for a solution with the surface boundary of the adjacent plume, which is represented as quadric expression. If the line of sight intersects the adjacent plume, the scattering, absorption, and re-emission of the bundle is simulated, and the bundle is tracked in that plume as previously described. In this manner, the influence of the dual plumes on one anothers' radiation field is simulated.

Surface Geometry Package

When the energy bundle escapes the boundaries of both plumes, it must be determined whether the line of sight intersects a Space Shuttle surface. To expedite this, the Space Shuttle surfaces are represented as quadric surfaces or planar surfaces. The surfaces of the cylinder, cone, sphere, ellipsoid, paraboloid, parellelogram, and disk may be represented by the quadric formula

$$C_1 X_1^2 + C_2 X_2^2 + C_3 X_3^2 + C_4 X_1 X_3 + C_5 X_2 X_3 + C_6 X_1 X_2 + C_7 X_1 + C_8 X_2 + C_9 X_3 + C_{10} = 0 \tag{27}$$

where X_1, X_2, X_3 represent the principal coordinate system centered equidistant between the SRB nozzles. $C_1, C_2, \ldots$ are the coefficients that determine the geometry of the surface. A detailed discussion on how these surfaces are described in functional form is found in Ref. 11. Each quadric surface may be subdivided along its principal axis. The surfaces may be grouped to simulate Space Shuttle geometries.

The line of sight of an energy bundle leaving the dual SRB plumes is written for the principal coordinate system in parametric form as

$$X_1 = X' + u_1 \cdot d \tag{28a}$$

$$X_2 = X'' + u_2 \cdot d \tag{28b}$$

$$X_3 = X''' + u_3 \cdot d \tag{28c}$$

Equation (28) is checked for a solution with expressions of Eq. (27) which represent each quadric surface used to simulate a Space Shuttle geometry. If a solution exists for Eq. (28) with any of the quadric expressions for the surfaces, the line of sight intersects the surface, and the energy contained in the bundle will contribute to the radiant heating of a subdivision on the surface. However, the line of sight may intersect several surfaces. In this case, the magnitudes of the vectors from the point where the bundle leaves the plume to the intersected surfaces are compared. The surface that has the shortest connecting vector absorbs the energy in the bundle and, in effect, shades all other surfaces along the line of sight. In this manner, surface shading is accounted for. The number of energy bundles striking each quadric surface subdivision is tallied, and the number of bundles hitting a surface is proportional to the radiant heat flux incident on the surface [Eq. (7)].

Results from SRB Thermal Radiation Model

The thermal radiation model discussed has the capability to predict the influence of plume flowfield structure on the distribution of thermal radiation leaving the plume. A major parameter affecting plume structure is the influence of altitude. Conditions at various trajectory points, principally M_∞, p_∞, and p_c, have significant effects on plume flowfield structure and plume expansion. The influences of these parameters (as defined by the SRB flowfield computational capability in Ref. 1) on plume flowfield structure have been documented in graphical and tabular form in Ref. 12. These data have been used in conjunction with the thermal radiation model described in this paper to predict the influence of altitude on the thermal radiation incident on the base plane of the Space Shuttle. The base plane is coincident with the nozzle exit plane and is at right angles to the plume axis at zero gimbal.

The influence of altitude on thermal radiation from one SRB plume incident on the base plane is shown in Fig. 4 for five nominal Space Shuttle trajectory points. M_∞, p_∞, and p_c for the five trajectory points are summarized in Table 1. The flowfield calculation for the sea-level trajectory point includes an afterburning simulation, as described in Ref. 13. The radiant heat fluxes shown in Fig. 4 extend to six nozzle exit radii away from the plume axis. The SRB model indicates that the radiant heat flux from a single SRB plume increases with altitude across the base plane up to an altitude of about 42,000 ft. Above 42,000 ft, the radiant heat fluxes decrease with altitude, decreasing more rapidly at larger distances from the plume axis.

Figure 5 shows the radiant fluxes for the 72,000-ft trajectory point for the base plane and for a plane at right angles to the plume axis and passing through the center of the aft dome of the external tank (ET) of the Space Shuttle. These data indicate that the radiant heating at the center of the aft dome of the ET from a single SRB plume is approximately 1.5 Btu/ft^2-sec.

Table 1 Nominal Space Shuttle ascent trajectory point data

Altitude (ft)	M_∞	P_∞ (psia)	P_c (psia)	Symbol Used in Fig. 4
Sea Level	0.0	14.7	763	○
9,430	0.6	10.4	682	□
24,000	1.05	5.8	544	◇
42,000	1.5	2.6	545	△
72,000	2.5	0.6	593	○
136,000	4.4	0.03	250	◊

Substantial difference of heat flux on left and right SRB structures is evident in the difference in magnitudes of the surface average and locally maximum heat fluxes.

Radiant heat fluxes from both SRB plumes across the aft dome of the ET and the SRB nozzle, shroud, and casing shown schematically in Fig. 6 are tabulated in Table 2. The numerals in Fig. 6 indicate the surface number corresponding to the heating rates given in Table 2. For convenience, the heat fluxes shown in Table 2 include a value averaged over the subsurface as well as the maximum local heat flux calculated

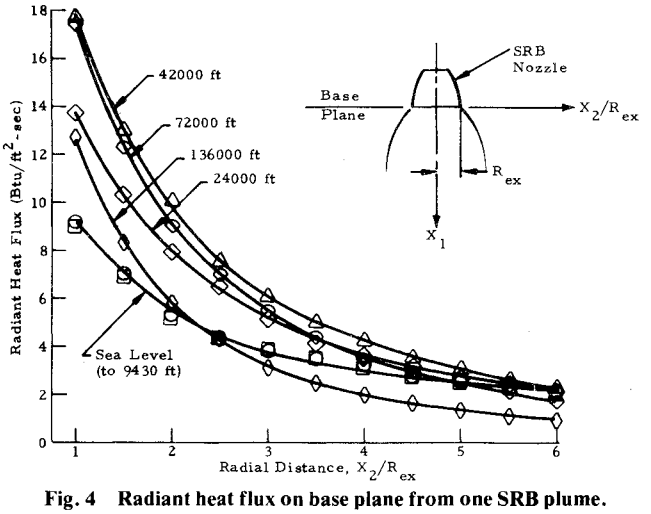

Fig. 4 Radiant heat flux on base plane from one SRB plume.

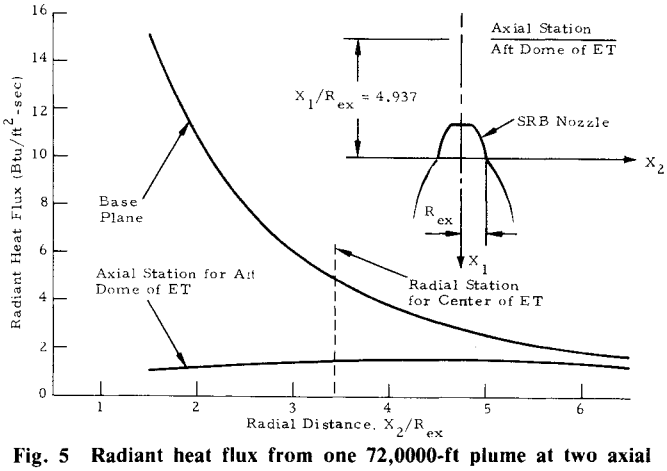

Fig. 5 Radiant heat flux from one 72,0000-ft plume at two axial locations.

Table 2 Radiant heat flux from both SRB plumes on SRB structures and ET at 9430 ft

Area	Heat Flux (Btu/ft^2-sec) Case 1	Case 2	Case 3
1a	0.50 (0.75)	0.62 (0.92)	0.56 (0.86)
1b	0.70 (1.01)	0.68 (0.95)	0.69 (0.89)
1c	0.88 (1.08)	1.04 (1.65)	1.03 (1.29)
1d	1.12 (1.27)	1.08 (1.52)	1.31 (1.61)
3	0.58 (2.15)	0.58 (2.00)	0.56 (2.00)
4	0.50 (1.82)	0.60 (1.96)	0.55 (1.78)
4b	1.99 (4.49)	2.02 (3.88)	1.45 (3.67)
6	0.58 (2.15)	0.58 (2.00)	0.77 (2.67)
7	0.50 (1.82)	0.60 (1.96)	0.46 (1.82)
7b	1.99 (4.49)	2.02 (3.88)	1.99 (3.67)
Pitch (deg)	0	9	0
Yaw (deg)	0	0	9

Table 3 Radiant heat fluxes on concentric rings on disks 1 and 2[a]

Disk 1	Mean Radius to Ring (in.)	Heat Flux (Btu/ft^2-sec)		
		9430 ft Alt.	72,000 ft Alt.	136,000 ft Alt.
Ring 1	60.45	0.09 (0.36)	1.26 (2.45)	0.74 (1.43)
Ring 2	77.93	1.23 (1.70)	3.59 (4.15)	2.08 (3.04)
Ring 3	95.41	2.24 (3.00)	4.88 (5.79)	3.09 (3.47)
Disk 2				
Ring 1	61.69	0.40 (2.4)	1.94 (4.36)	0.64 (1.70)
Ring 2	64.38	0.57 (2.3)	1.75 (4.19)	0.95 (2.45)
Ring 3	67.00	0.0	1.12 (2.68)	1.37 (3.14)
Ring 4	69.63	1.06 (2.11)	1.61 (5.16)	1.45 (3.78)
Ring 5	72.25	0.17 (2.03)	2.70 (4.98)	0.91 (2.18)

[a] Numbers in parentheses indicate maximum flux within the ring.

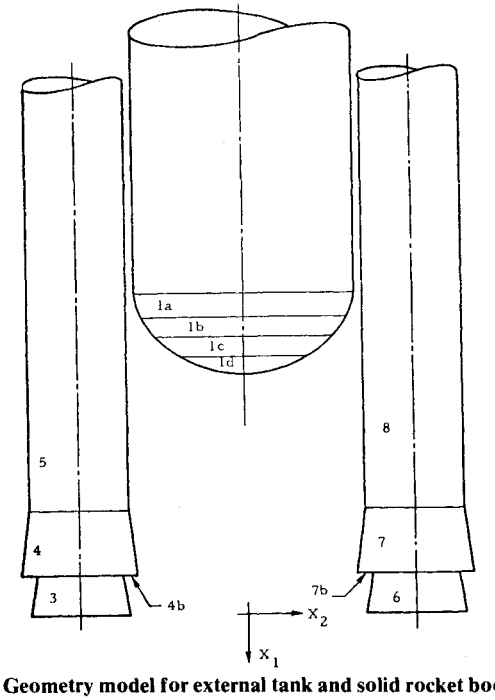

Fig. 6 Geometry model for external tank and solid rocket boosters.

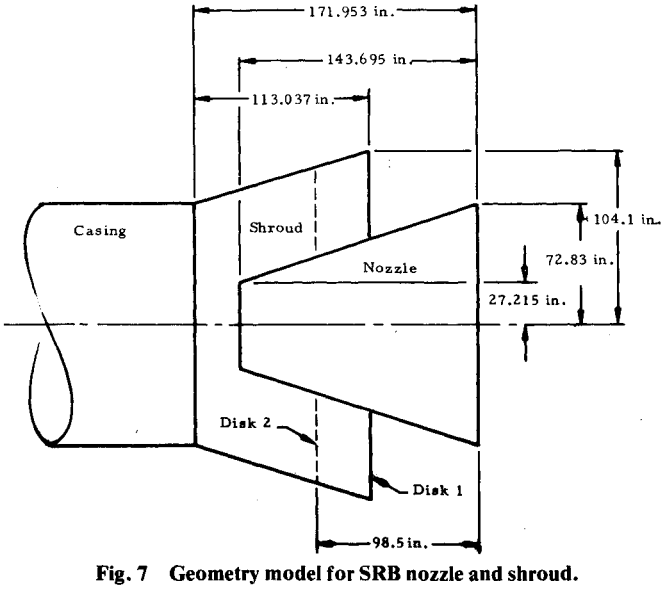

Fig. 7 Geometry model for SRB nozzle and shroud.

for the surface. The maximum flux occurs on the subsurfaces facing the plumes. Case 2 shows heat fluxes for a 9-deg gimbal angle in the pitch plane for both plumes. The heat fluxes are increased when both plumes are 9-deg gimbaled. Case 3 shows heat fluxes when both plumes are yawed 9 deg. The symmetry of heat flux no longer exists in the latter case.

Figure 7 shows a more detailed geometry model for the nozzle and shroud for the SRB. Averaged radiant heat fluxes from both SRB plumes to this geometry model are shown in Table 3 for altitudes of 9430, 72,000, and 136,000 ft. Disk 1 corresponds to a thermal shielding curtain. Disk 2 is situated at the midpoint of the nozzle gimbal actuator. Disks 1 and 2 are subdivided into three and five concentric rings, respectively. The concentric rings are numbered in increasing order outward from the nozzle wall.

The computer program has been quite efficient, and it requires moderate sample size for most cases. To define a plume surface accurately, a sample size of 100,000 energy bundles would be generated and stored on a magnetic tape. The computer processor time required for such a case would range from 30 to 70 min on the Univac 1108 system, depending on plume altitude. In other cases, the sample size and computer time depend on the complexity of the target geometry.

Radiant heat fluxes predicted by the SRB thermal radiation model are lower than those predicted by view factor calculations used in conjunction with a uniform plume emissive power. The view factor methodology is presently being used to generate SRB plume base heating environments for design of thermal protection systems for the Space Shuttle. In this methodology, the SRB plume is simulated as a conical diffuse surface (half-cone angle typically assumed to be 15 deg) with a plume surface emissive power of 40 Btu/ft^2-sec (including a safety factor of 1.6), which matches experimental flight base heating data fairly well.[14] Since a safety factor is used in present design calculations of SRB thermal radiation and the plume is assumed to be a diffuse surface, it is expected that the radiant heat fluxes predicted by SRB plume thermal radiation model described in this paper will be lower.

Conclusions

The thermal radiation model discussed in the foregoing provides the capability to calculate SRB plume radiant heat fluxes to the base region of the launch vehicles as influenced by plume flowfield structure. The magnitudes of thermal radiation are calculated based on coupled radiation from Al_2O_3 particles and the principal emitting gases (CO, CO_2, H_2O, and HCl), which are modeled as gray media under

conditions of local thermodynamic equilibrium. The dispersion of Al_2O_3 particles and gases may have axial and radial variations such that actual SRB flowfield structures may be approximated. The ability to consider plume flowfield structure makes it possible to determine the influences of such parameters as altitude, chamber pressure, trajectory point, etc., on SRB thermal radiation once a flowfield definition is available. The magnitudes of radiant heat fluxes predicted by the model tend to be lower than those predicted through use of a view factor calculation and an empirically determined plume emissive power.

Acknowledgment

This work was supported in part by NASA contracts NAS8-31310 and NAS8-28609 under the direction of W.C. Claunch and T.F. Greenwood of the Marshall Space Flight Center.

References

[1] Stockham, L.W. and Love, T.J., "Radiative Heat Transfer from a Cylindrical Cloud of Particles," *AIAA Journal,* Vol. 6, Oct. 1968, pp. 1935-1940.

[2] Watson, G.H., Logan, N.A., and McAnally, J.V., "Prediction of Radiation Heat Transfer Characteristics from Solid Rocket Plumes Using the Monte Carlo Technique," Lockheed Missiles & Space Co., Huntsville, Ala., LMSC-HREC TM D306995, Jan. 1974.

[3] Watson, G.H., Audeh, B.J., and Farmer, R.C., "Radiation Heating from Solid Motor Plumes," *8th JANNAF Plume Technology Meeting,* U.S. Air Force Academy, Colorado Springs, Colo., July 1974.

[4] Watson, G.H. and Lee, A.L., "Solid Rocket Booster Thermal Radiation Model—Vol. I—Final Report," Lockheed Missiles & Space Co., Huntsville, Ala., LMSC-HREC TR D496763-I, March 1976.

[5] Penny, M.M., Smith, S.D., Anderson, P.G., Sulyma, P.R., and Pearson, M.L., "Supersonic Flow of Chemically Reacting Gas-Particle Mixtures," Lockheed Missiles & Space Co., Huntsville, Ala., LMSC-HREC TR D4966555, Jan. 1976.

[6] Abu-Romia, M.M. and Tien, C.L., "Appropriate Mean Absorption Coefficients for Infrared Radiation of Gases," *Journal of Heat Transfer,* Nov. 1967, pp. 321-327.

[7] Laderman, A.J. and Carlson, D.J., "Radiation from Particle Laden Plumes," Air Force Rocket Propulsion Laboratory, AFRPL-TR-67-223, Vol. II, 1967.

[8] Howell, J.R. and Perlmutter, M., "Monte Carlo Solution of Radiant Heat Transfer in a Non-Gray Nonisothermal Gas with Temperature Dependent Properties," *American Institute of Chemical Engineers Journal,* July 1964.

[9] Howell, J.R., "Calculation of Radiant Heat Exchange by the Monte Carlo Method," *Winter Annual Meeting of the ASME,* Paper 65 WA/HT-54, Nov. 7-11, 1965.

[10] Tien, C.L. and Abu-Romia, M.M., "Radiative Energy Transfer to Outer Base Regions of Cylindrical and Conical Gas Bodies," Inst. of Engineering Research, Univ. of California, Berkeley, Calif., 1963, Rept. AS-63-4.

[11] Paoletti, C.J., Pond, J.E., and Vance, J.H., "Determination of Quadric Equation Coefficients Describing Three-Dimensional Surfaces," NASA Tech. Support Package, TSP 69-10435, Sept. 1969.

[12] Smith, S.D., "Space Shuttle Solid Rocket Motor (SRM) Exhaust Plume Definitions—Sea Level to SRB Separation," Lockheed Missiles & Space Co., Huntsville, Ala., LMSC-HREC TM D496879, Aug. 1976.

[13] Audeh, B.J. and Smith, S.D., "Space Shuttle Solid Rocket Motor and Orbiter Main Engine Plumes at Sea Level," Lockheed Missiles & Space Co., Huntsville, Ala., LMSC-HREC TN D390419, Oct. 1974.

[14] Kramer, O.G., "Evaluation of Thermal Radiation from the Titan III Solid Rocket Motor Exhaust Plumes," AIAA Paper 70-842, Los Angeles, Calif., July 1970.